

Nonlinear variations in the electronic structure of II–VI and III–V wurtzite semiconductors with biaxial strain

Shenyuan Yang,^{a)} David Prendergast, and Jeffrey B. Neaton^{b)}
*Molecular Foundry, Lawrence Berkeley National Laboratory, 1 Cyclotron Road, Berkeley,
 California 94720, USA*

(Received 25 February 2011; accepted 22 March 2011; published online 14 April 2011)

Using first-principles calculations within many-body perturbation theory, we predict effects of biaxial strain on electronic band gaps and band edges of wurtzite III–V and II–VI semiconductor compounds. We find strain-induced changes in band gaps are large and highly nonlinear. Under both compressive and tensile biaxial strains, II–VI chalcogenide band gaps are predicted to decrease by as much as 0.6 eV for 10% strain; in contrast, III–V nitrides attain maximum gaps for compressive strains near 4%. Whereas nitrides tend to preserve covalent bond angle, more ionic chalcogenides tend to preserve bond length and volume, leading to qualitatively different trends in electronic structure. © 2011 American Institute of Physics. [doi:10.1063/1.3578193]

Semiconductor heterojunctions, such as quantum wells¹ and multicomponent nanostructures,² have attracted tremendous attention over recent decades for their potential as active components in electronic, optoelectronic, and light-harvesting devices. In planar thin film and superlattice geometries, large anisotropic strain (as much as 5% or more³) can result from the often-significant lattice mismatch between materials and/or the substrate. Similarly, heterojunctions in semiconducting nanorods and core-shell nanoparticles can potentially remain coherent at even larger lattice mismatch.^{2,4} These large strains can have significant effects on band gaps and related electronic properties, and in nanoscale systems, the change in band gap induced by strain is of similar magnitude to that induced by quantum confinement effects.⁵ Traditionally, energies associated with near-gap band structure have been described as linear functions of the strain tensor.^{6–8} At relatively small strain (e.g., $\pm 2\%$), strain-induced shifts in energies and band gaps do behave linearly.⁸ At larger strain, prior first-principles calculations have predicted nonlinearities under biaxial and uniaxial strains for several related compounds.^{9,10} However, a general understanding of the effect of anisotropic strain on electronic structure of wurtzite compounds is still lacking.

In this letter, using density functional theory (DFT) and many-body perturbation theory within the GW approximation, we show that both the trends in band gap and band edge energies of wurtzite III–V and II–VI semiconductors are highly nonlinear over a wide range of biaxial strain (up to 10%), with predicted reductions in gaps of up to 1.5 eV and 0.6 eV for III–V and II–VI materials, respectively. We predict that while the band gap of II–VI chalcogenides always decreases with biaxial strain, the band gap of III–V nitrides grows initially up to 4% compressive strain. Combined with recent experimental strategies^{3,4} to achieve high strain in semiconductor materials, our calculations will aid in the design lattice-mismatched heterojunctions with desirable optoelectronic properties.

Throughout this letter, all lattice parameters are optimized with DFT as implemented in the Vienna *ab initio*

simulation package (VASP) (Ref. 11) and the generalized-gradient approximation of Perdew, Burke, and Ernzerhof (PBE).¹² We employ projector-augmented wave¹³ potentials and a $12 \times 12 \times 12$ Monkhorst–Pack mesh for k-point sampling.¹⁴ A plane-wave cutoff of 300 eV for II–VI chalcogenides and 450 eV for III–V nitrides, respectively, results in good convergence of all properties described here. The PBE lattice constants for equilibrium CdSe (GaN) are $a_0 = 4.395$ (3.216) Å, and $c_0 = 7.178$ (5.240) Å, $\sim 2\%$ (1%) larger than experiment.¹⁵

To obtain reliable band gaps, we use many-body perturbation theory within the GW approximation.¹⁶ In these calculations, DFT Kohn–Sham eigenvalues are perturbatively corrected by a GW self-energy, itself computed from a generalized Kohn–Sham system. Thus, GW self-energy corrections depend on the initial Kohn–Sham system. For this work, we explored wave functions and eigenvalues calculated with PBE, hybrid HSE03,¹⁷ and HSE06¹⁸ functionals for bulk GaN and CdSe at experimental and computed equilibrium lattice parameters. The details of the GW calculations are similar¹⁹ appear in [Ref. 20]. We find that at the PBE lattice parameters, the band gaps from a one-shot G_0W_0 calculation on top of HSE03 exhibit the best agreement with experimental gaps¹⁵ (see Table SI in Ref. 21). This comparison is acceptable given that exciton binding energies are < 0.1 eV in these compounds. We find that the trends in gaps under biaxial strain are similar from different levels of calculations.²¹ HSE03+ G_0W_0 is used for band gaps for the remainder of this study (and PBE+ G_0W_0 for band edges, where G refers to an updated Green's function).

We consider a wide range of biaxial strain (up to $\pm 10\%$) perpendicular to the c axis (and assuming epitaxial growth along [0001]). We model strained films and junctions using periodic bulk calculations in which the in-plane lattice parameter a is constrained while the normal axis c and atomic positions are fully relaxed, neglecting quantum confinement effects associated with thin films that may provide an additional contribution to the band gap.⁵ In Fig. 1, we show the strain-induced changes in the band gaps of five wurtzite compounds. Under tensile strain, the gaps decrease with increasing a . For II–VI chalcogenides, the gaps also decrease with decreasing a [Fig. 1(b)], with a maximum near equilib-

^{a)}Electronic mail: syang4@lbl.gov.

^{b)}Electronic mail: jboneaton@lbl.gov.

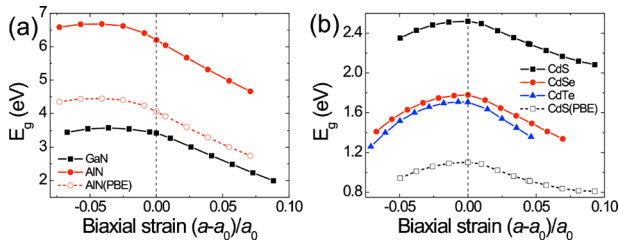


FIG. 1. (Color online) The energy band gaps of (a) III-V GaN and AlN, (b) II-VI CdS, CdSe, and CdTe compounds as a function of biaxial strain in (0001) plane calculated from HSE03+ G_0W_0 . The band gaps of AlN and CdS from PBE are also shown for comparison.

rium. In contrast, the gaps of the nitrides first increase and then decrease with decreasing a [Fig. 1(a)], exhibiting highly nonlinear trends with biaxial strain. The maximum band gaps are at -3.5% and -4.1% for GaN and AlN, respectively.

The trends in band gap with biaxial strain can be understood by considering the band edges. We calculate the absolute energies of the band edges with respect to the common vacuum level, using the average potential as reference energy. We employ a two-step approach to define the vacuum level. First, for a particular strained system we determine the relative positions of the band edges with respect to the average potential (the reference energy) from a bulk calculation. Second, we construct a thick slab with the same strain and calculate the average potential in the center of the slab with respect to the vacuum level. Then we reference the band edges relative to the vacuum level which is a common energy zero in all calculations. This approach is necessary because the reference energy is not constant under strain and serves only as an intermediate step to align the band edges relative to the vacuum level. Previous approaches ignore the deformation potential of the deep core levels and use them as reference energy,^{9,10} which has been recognized as problematic.²²

The computed absolute energies of band edges of GaN and CdSe are shown in Fig. 2. To avoid the computational demands of a slab calculation with hybrid functionals, all numbers are obtained with PBE+ GW_0 approximation. The conduction band minimum (CBM), an antibonding s -state at Γ , decreases with increasing a , and the valence band maximum (VBM) changes its character under biaxial strain. At equilibrium, the wurtzite structure is not perfectly tetrahedral with nonideal c/a and u , and the VBM consists of near-degenerate heavy hole (HH) and crystal-field-split hole (CH) bands, with the CH band just below the HH band at the Γ point [Fig. 3(a)]. (Note that we neglect spin-orbit splitting of the HH band.) The only exception is AlN where the CH is above the HH band.²³ Under compressive biaxial strain, the

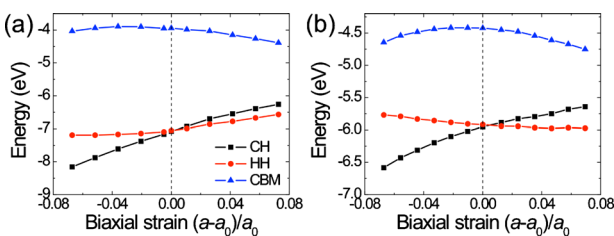


FIG. 2. (Color online) The absolute energies with respect to vacuum of relevant energy bands (CBM, CH, and HH) of (a) GaN and (b) CdSe as a function of biaxial strain in (0001) plane.

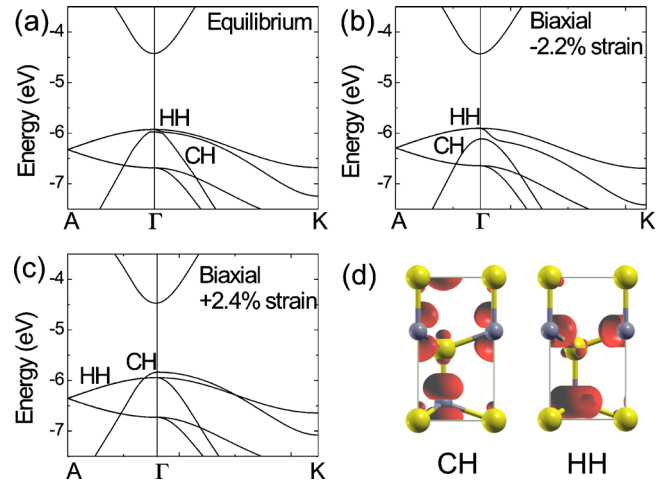


FIG. 3. (Color online) The band structures along A- Γ -K near the Fermi level of CdSe at (a) equilibrium, (b) biaxial compressive strain of -2.2% , and (c) biaxial tensile strain of $+2.4\%$ in (0001) plane. The CH and HH bands are highlighted for comparison. (d) The CH and HH states of wurtzite CdSe at equilibrium.

CH band shifts downward, increasing the HH-CH splitting [Fig. 3(b)]. Under tensile strain, the CH band shift upward and becomes the VBM [Fig. 3(c)]. Note that under isotropic strain, the energetic ordering of band edges is similar to equilibrium, and the band gap and energy levels increase linearly under compression, an effect well described by the volume deformation potentials.⁶

The HH band is always at the Γ point. At large tensile biaxial strain, CH band maximum shifts slightly away from the Γ in the xy plane. We observe a direct-to-indirect transition at 5.7% and 3.5% tensile strain for CdS and CdSe, respectively, and at a much higher (15%) tensile strain for GaN. At extremely high tensile strains (e.g., 10% for CdSe), there is a transition to a pseudographitic phase,²⁴ where the cations become coplanar with the anions. Associated with the structural transition, the band maximum at H becomes the VBM, resulting in a sudden decrease in the band gap. Since this VBM state has different character, we will not consider the pseudographitic phase further in our study.

To understand the trends in the band edges with strain, we plot the wurtzite structural parameters in Fig. 4. In the unstrained wurtzite primitive cell, each cation is coordinated by four anion neighbors and vice versa. The two inequivalent bond lengths d_1 (axial bond) and d_2 (nonaxial bond) between neighbors are determined by the lattice parameters u and c/a . Compressive biaxial strain results in increase in c and

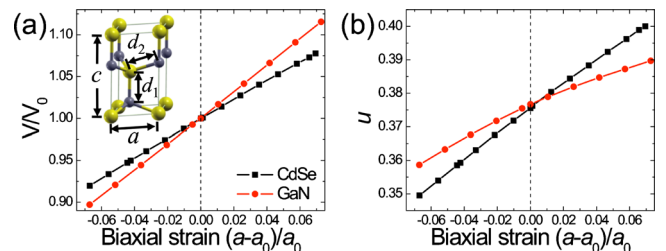


FIG. 4. (Color online) The changes in (a) the volume of the unit cell and (b) the internal parameter u as a function of biaxial strain in (0001) plane for wurtzite CdSe and GaN. The inset in (a) shows the wurtzite unit cell and the structural parameters. The Cd and Se atoms are represented by large and small balls, respectively.

d_1 , and a slight overall decrease in volume [Fig. 4(a)]. Concomitantly, the internal parameter u also decreases [Fig. 4(b)], reducing the difference between d_1 and d_2 (partially restoring tetrahedral-like coordination), and we still have $d_1 > d_2$ (Fig. S2 in Ref. 21). Under tensile strains, u , d_1 , and d_2 all increase with increasing a , but $d_1 < d_2$. Under isotropic strain, u remains relatively unchanged, near-tetrahedral coordination is maintained, and the energetic ordering and symmetry of the electronic structure is preserved.

Interestingly, the more covalent III–V nitrides respond to strain differently from the more ionic II–VI chalcogenides. III–V nitrides tend to preserve the direction of the covalent bonds around each atom under strain, at the expense of changes in bond length and volume. In contrast, the II–VI chalcogenides tend to preserve bond length and volume and are more flexible in the bond angles. Therefore, at a given biaxial strain the u parameter in GaN is closer to the ideal $u_0 = 3/8$ compared to CdSe, and GaN exhibits a larger change in volume (see Fig. 4). These detailed differences in structure lead to different trends in the change in band gap under biaxial strain between nitrides and chalcogenides as we now discuss.

For both CdSe and GaN, the volume of the unit cell and bond lengths grow with increasing a , leading to a reduced energy for antibonding s states. Therefore, the CBM decreases under tensile strain, and initially increases under compressive strain, as shown in Fig. 2. Since the CBM attains p_z character under these strains, bonding interactions eventually reduce the energy of the CBM at large compressive strain (larger than 3.5%). The p_z -like CH band originating with out-of-plane coupling [Fig. 3(d)], and p_x - and p_y -like HH bands (in-plane coupling, [Fig. 3(d)], exhibit different trends. Under compressive strain, d_2 decreases faster than d_1 ($d_1 > d_2$), and the in-plane p_x - p_y coupling is enhanced relative to out-of-plane, resulting in a larger band width and a higher energy of the HH band (relative to CH). The opposite trend is found under tensile biaxial strain.

From Fig. 2, the details of the HH band edge evolution are system-dependent. Under compressive strains, the HH edge decreases in GaN, but increases in CdSe. The larger decrease in bond angles induced by compressive strain in CdSe increases the in-plane coupling and the HH band energy. The more covalent GaN, on the other hand, incurs a larger change in volume with strain, reducing the average energy of bonding bands. Therefore, the HH band energy in CdSe increases under compressive strain, while in GaN it exhibits the opposite trend although the change is small (Fig. 2).

The trends in the band gaps of strained wurtzite compounds (Fig. 1) can thus be understood as follows. Under tensile biaxial strain, the gap always decreases, since the CBM energy declines and the VBM (CH) energy rises. Under compressive biaxial strain, the competition between the CBM and VBM (HH) results in different trends in nitrides and chalcogenides. For small-to-moderate compressive strains (less than 3.5%), the CBM position increases and the HH energy decreases slightly [Fig. 2(a)] in nitrides, resulting in an increase in the gap. At larger compressive strains, the

CBM energy decreases due to a growing p_z bonding contribution, and the GaN gap reaches a maximum and begins to drop with compression. For CdSe, conversely, the CBM energy always increases more slowly than that of the HH [Fig. 2(b)], resulting in an overall decrease in the gap under compression for all biaxial strains considered.

In summary, quantitative first-principles many-body perturbation theory calculations predict that wurtzite III–V and II–VI semiconductor compounds exhibit highly nonlinear trends in the band gaps and band edges under biaxial strain. Our study improves the understanding of the electronic structure of semiconductors and lattice-mismatched heterojunctions under large anisotropic strain, where linear response theories and standard ground-state DFT are insufficient to describe the trends in energy levels.

This work was performed at the Molecular Foundry and within the Helios Solar Energy Research Center, both supported by the Office of Science, Office of Basic Energy Sciences, of the U.S. Department of Energy under Contract No. DE-AC02-05CH11231. All calculations were performed on the Nano and Vulcan compute clusters at LBNL and on Franklin at NERSC.

- ¹S. Nakamura, T. Mukai, and M. Senoh, *Appl. Phys. Lett.* **64**, 1687 (1994).
- ²R. D. Robinson, B. Sadtler, D. O. Demchenko, C. K. Erdonmez, L.-W. Wang, and A. P. Alivisatos, *Science* **317**, 355 (2007).
- ³O. Husberg, A. Khartchenko, D. J. As, H. Vogelsang, T. Frey, D. Schikora, O. C. Noriega, A. Tabata, and J. R. Leite, *Appl. Phys. Lett.* **79**, 1243 (2001).
- ⁴A. M. Smith, A. M. Mohs, and S. Nie, *Nat. Nanotechnol.* **4**, 56 (2009).
- ⁵S. Yang, D. Prendergast, and J. B. Neaton, *Nano Lett.* **10**, 3156 (2010).
- ⁶R. Resta, *Phys. Rev. B* **44**, 11035 (1991).
- ⁷S. L. Chuang and C. S. Chang, *Phys. Rev. B* **54**, 2491 (1996).
- ⁸J.-M. Wagner and F. Bechstedt, *Phys. Rev. B* **66**, 115202 (2002).
- ⁹P. R. C. Kent, G. L. W. Hart, and A. Zunger, *Appl. Phys. Lett.* **81**, 4377 (2002).
- ¹⁰E. S. Kadantsev, M. Zielinski, M. Korkusinski, and P. Hawrylak, *J. Appl. Phys.* **107**, 104315 (2010).
- ¹¹G. Kresse and J. Furthmüller, *Phys. Rev. B* **54**, 11169 (1996).
- ¹²J. P. Perdew, K. Burke, and M. Ernzerhof, *Phys. Rev. Lett.* **77**, 3865 (1996).
- ¹³P. E. Blöchl, *Phys. Rev. B* **50**, 17953 (1994).
- ¹⁴H. J. Monkhorst and J. D. Pack, *Phys. Rev. B* **13**, 5188 (1976).
- ¹⁵*Landolt-Börnstein: Numerical Data and Functional Relationships in Science and Technology, New Series*, edited by W. Martienssen (Springer, New York, 1982), Vols. 41a1a-41a1b and 42b.
- ¹⁶M. S. Hybertsen and S. G. Louie, *Phys. Rev. B* **34**, 5390 (1986).
- ¹⁷J. Heyd, G. E. Scuseria, and M. Ernzerhof, *J. Chem. Phys.* **118**, 8207 (2003).
- ¹⁸A. V. Kravau, O. A. Vydrov, A. F. Izmaylov, and G. E. Scuseria, *J. Chem. Phys.* **125**, 224106 (2006).
- ¹⁹M. Shishkin and G. Kresse, *Phys. Rev. B* **75**, 235102 (2007).
- ²⁰In the GW calculations, we used an $8 \times 8 \times 8$ k-point grid centered at the Γ point and 50 frequency points. The total number of bands is 200. The energy cutoff for response function is half of cutoff of plane wave basis in the ground-state PBE calculation.
- ²¹See supplementary material at <http://dx.doi.org/10.1063/1.3578193> for comparison of band gaps from different calculations and details of structural parameters under strain.
- ²²Y.-H. Li, X. G. Gong, and S.-H. Wei, *Appl. Phys. Lett.* **88**, 042104 (2006).
- ²³M. Suzuki, T. Uenoyama, and A. Yanase, *Phys. Rev. B* **52**, 8132 (1995).
- ²⁴S. K. Yadav, T. Sadowski, and R. Ramprasad, *Phys. Rev. B* **81**, 144120 (2010).